ISSN 1330-3651 (Print), ISSN 1848-6339 (Online) https://doi.org/10.17559/TV-20210728035851
Original scientific paper

A Dual Frequency Predistortion Adaptive Sparse Signal Reconstruction Algorithm

Mingming GAO, Shaojun FANG*, Jinling WANG, Xueman ZHANG, Yuan CAO

Abstract: To solve the problem of a high sampling rate in the dual-frequency power amplifier predistortion system, a dual frequency predistortion adaptive sparse signal reconstruction algorithm is proposed. Firstly, a memory effect compensator based on piecewise polynomial model is adopted. The signal fusion is interpreted as the problem of Compressed Sensing sampling reconstruction. In the predistortion feedback loop, the missing fifth-order and high-order cross-modulation signals are reconstructed accurately by using the adaptive sparse algorithm. The minimum mean square solution of coefficient weight approximates the optimal value, and the acquisition error is reduced to improve the linearization effect. The experimental results show that it is of great significance to reduce the sampling rate of dual band predistortion and improve the linearity of power amplifier.

Keywords: adaptive reconstruction algorithm; compressed sensing; dual frequency amplifier; predistortion; subspace tracking

1 INTRODUCTION

Intelligent, multi-frequency [1] and low energy consumption of modern communication systems make the efficient use of radio spectrum resources get more attention. Digital Predistortion (DPD) [3] is a linearization method of the Radio Frequency Power Amplifier (RF PA) in the multi-carrier communication system. It has aroused wide concern from domestic and foreign experts because of its high precision and good stability.

In the research of dual-frequency digital predistortion system [4], Roblin et al. of Ohio State University used the Large Signal Network Analyzer (LSNA) to obtain power amplifier parameters and extract predistorter coefficients, and proposed a frequency selective predistortion structure [5] in 2008. In 2012, Kim Jhwo and others extended the predistortion structure to the fifth order [6], and achieved ideal linearization effect. Cidronali of the University of Florence applied an undersampling receiver in the feedback loop and proposed an intermediate frequency digital pre-distortion (IF-DPD) [7]. Bassam [8] and other people performed nonlinear predistortion compensation on two separated frequency bands, and proposed two-dimensional digital predistortion. However, the sampling rate of Analog-to-Digital Converter (ADC) is severely limited in the feedback loop of a dual-frequency predistortion system [9]. Compressed Sensing (CS) [10] technology has been widely used in predistortion in recent years, which can reduce the sampling rate on the RF front-end effectively. CS theory is different from the traditional Nyquist sampling theorem. In signal sampling, it is no longer necessary to process all N-dimensional signals, but to measure linearly with the M-dimensional observation matrix which is much smaller than N.

In this paper, a dual-frequency under-sampling predistortion system based on compressed sensing is proposed. Firstly, a memory effect compensator based on piecewise linear function dual-frequency power amplifier predistortion model is established, and then the compressed sensing adaptive sparse reconstruction algorithm is applied to the predistortion system feedback loop. The Information compression sensing sensor is sampled in the predistortion feedback loop, and the fifth-order and high-order intermodulation signals are reconstructed by the APSP (Adaptive Sparse algorithm). According to the characteristics of the feedback loop gnal itself, the algorithm dynamically adjusts the sparsity starting value and the step size to approximate the true sparsity and then uses subspace pursuit. A tracking algorithm is used to enhance the coefficient estimation weight and improve the predistortion effect by reducing the signal with high accuracy. According to the characteristics of feedback loop signals, the algorithm dynamically adjusts the initial value and step size of sparsity to approximate the true sparsity. Then the subspace tracking algorithm is used to restore the signal accurately, to improve the coefficients estimation weight and the predistortion effect. This method combines the low complexity power amplifier model with the under-sampling dual-frequency predistortion structure, which reduces the sampling rate compared with the traditional predistortion. Compared with 2D-Memory Polynomial (2D-MP), 2D-Dynamic Deviation Reduction (2D-DDR), and 2D-Canonical Piecewise Linear (2D-CPWL), Normalized Means Squared Error (*NMSE*) increased by about 2 – 3 dB. If the *ACPR* (Adjacent Channel Power Ratio) needs to be improved to 49 dB, the output power only needs to be back about 1 dB, closing to the ideal linear power amplifier, which can be widely used in the development of multi-band communication.

1.1 Power Amplifier Model and Five Order Equal High Order Intermodulation Spectrum Analysis

The CPWL function can be used to accurately fit the nonlinear behavior of strongly nonlinear systems [11-12]. When the memory effect is considered, the piecewise linear function has the following expression [13].

$$y(n)=\sum_{i=0}^{M}a_i x(n-i)+b+\sum_{\mathrm{r}=1}^{R}b_r\left|\sum_{i=1}^{M}\delta_{ri}x(n-i)-\beta_r\right| \quad (1)$$

$x(n)$ and $y(n)$ are input and output of nonlinear systems respectively. a_i , b_{r} and δ_{ri} are the coefficients of piecewise linear functions. b stands for DC bias and can be ignored in digital predistortion. Linear b stands for DC bias and can be ignored in digital predistortion. M represents the memory depth of the model,

and R represents the segment number of the piecewise linear function. $\beta_r = r/R$ represents the threshold used to define the boundary of piecewise linear functions.

According to reference [13], after the lattice is segmented and the DC bias term is omitted, the Eq. (1) can be transformed into a linear relationship between the output and the coefficient:

$$\mathrm{y}(n)=\sum_{i=0}^{M} a_i \mathrm{x}(n-i)+\sum_{r=1}^{R}\sum_{i=1}^{M} b_r \left|x(n-i)\right| e^{\mathrm{j}\theta(n-i)} \quad (2)$$

$\theta(n-i)$ is the phase of $\mathrm{x}(n-i)$. $\mathrm{x}_1(n-i)e^{\mathrm{j}\omega_1 \mathrm{t}}$ and $\mathrm{x}_2(n-i)e^{\mathrm{j}\omega_2 \mathrm{t}}$ are defined as input signals of frequency one and frequency two, respectively, with center frequencies $\omega_1 = 2\pi f_1$ and $\omega_2 = 2\pi f_2$ assuming $(\omega_2 > \omega_1)$. $\mathrm{x}_1(n-i)$ and $\mathrm{x}_2(n-i)$ represents the complex envelope of the base band. When $\omega = (\omega_2 - \omega_1)/2$, the dual frequency baseband equivalent signal in discrete time domain is shown below [14]:

$$x(n) = x_1(n)e^{-j\omega n\mathrm{T}} + x_2(n)e^{j\omega n\mathrm{T}} \quad (3)$$

where $t = nT$, T is the sampling interval. Bring Eq. (3) into Eq. (2):

$$y(n) = y_1 + \mathrm{y}_2 \quad (4)$$

$$y_1(n)=\sum_{i=0}^{M} a_i \left[x_1(n-i)\mathrm{e}^{-jwnt} + x_2(n-i)\mathrm{e}^{-jwnt}\right] \quad (5)$$

$$y_2(n)=\sum_{\mathrm{r}=1}^{R}\sum_{i=0}^{M} b_{r,i} \left|x_1(n-i)\mathrm{e}^{-jwnt} + x_2(n-i)\mathrm{e}^{-jwnt}\right| - \beta_r \left|\mathrm{e}^{j\theta(n-i)}\right. \quad (6)$$

The input and output parameters of CPLW structure are both real domains, but the signals transmitted in the actual channel are complex signals. Therefore, the model still has the problem of conversion into the numerical domain. In Eq. (6), $\mathrm{x}(n-i)$ is a complex signal, $\left|\mathrm{x}(n-i)\right|$ is the amplitude of the complex signal, and $\theta(n-i)$ is the phase information of the complex signal. Although the model can accurately represent all the information of the signal, the model is too complicated because it involves the extraction and calculation of phase information.

The phase information in Eq. (6) is removed, and the $x_1(n-i)\mathrm{e}^{-jwnt} + x_2(n-i)\mathrm{e}^{-jwnt}$ is added to multiply the polynomial. The structure contains phase information, so the structure can represent the power amplifier model with nonlinear and memory effects. The CPLW is modified to eliminate the phase multiplied by the original input signal.

$$\mathrm{y}(n)=\sum_{i=0}^{M} a_i \left[x_1(n-i)\mathrm{e}^{-\mathrm{j}\omega \mathrm{nt}} + x_2(n-i)\mathrm{e}^{\mathrm{j}\omega \mathrm{nt}}\right] + b + \sum_{\mathrm{r}=1}^{R}\sum_{i=0}^{M} b_{r,i}\left[x_1(n-i)\mathrm{e}^{-\mathrm{j}\omega \mathrm{nt}} + x_2(n-i)\mathrm{e}^{\mathrm{j}\omega \mathrm{nt}}\right] \left|x_1(n-i)\mathrm{e}^{-\mathrm{j}\omega \mathrm{nt}} + x_2(n-i)\mathrm{e}^{\mathrm{j}\omega \mathrm{nt}}\right| - \beta_r \left|\mathrm{e}^{\mathrm{j}\theta(n-i)}\right. \quad (7)$$

1.2 Nonlinear System Structure and Five Order Intermodulation Signal

Fig. 1 is the structure of an indirect learning nonlinear system [15]. Assuming that the transmission function of the nonlinear system is $W(\mathrm{e}^{\mathrm{j}\omega})$. The main path X_n is defined as the input signal of the nonlinear system. The output of the nonlinear system is Y_n. In the branch, the input signal ∂_n is m_n. After the output of the inverse model, the coupling signal $(d_n = x_n)$ is subtracted from m_n. The inverse model coefficients are optimized by using error e_n. In order to correct the power spectral density of the equivalent nonlinear model of the power amplifier, that is, the third and fifth order intermodulation are not correlated with the input signal, the power spectrum of the input signal of the inverse model is as follows:

$$G_{\partial_1+\partial_2}(\mathrm{e}^{\mathrm{j}\omega}) = \left|W(\mathrm{e}^{\mathrm{j}\omega})\right|^2 G_{X_1+X_2}(\mathrm{e}^{\mathrm{j}\omega}) - G_{ff}(\mathrm{e}^{\mathrm{j}\omega}) \quad (8)$$

The input power spectral density of the inverse model is $G_{\partial_1+\partial_2}(\mathrm{e}^{\mathrm{j}\omega})$. The power spectral density of the missing fifth-order and equal-high-order intermodulation component is $G_{f_1+f_2}(\mathrm{e}^{\mathrm{j}\omega})$. The $W(\mathrm{e}^{\mathrm{j}\omega})$ is the transmission function of the nonlinear system. The input power spectral density of the nonlinear system is $G_{\mathrm{x}_1+\mathrm{x}_2}(\mathrm{e}^{\mathrm{j}\omega})$.

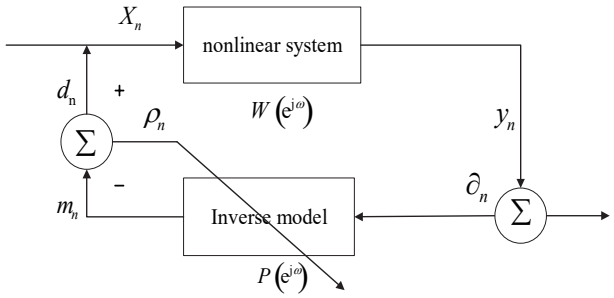

Figure 1 Adaptive system of the inverse model

In [15], the non-linear system is equivalent to the modified linear system and the modified non-linear system. Using the spectrum to demonstrate the ideal acquisition of the high-order intermodulation signals, the inverse model transfer function is approximated to the optimal transfer function when the power spectral density $G_{f_1+f_2}(\mathrm{e}^{\mathrm{j}\omega})$ is zero. However the bandwidth of the feedback loop is limited, it is difficult to achieve ideal acquisition. Therefore, $G_{f_1+f_2}(\mathrm{e}^{\mathrm{j}\omega})$ is not zero, that is to

say, in adaptive inverse simulation system, the missing fifth-order equal-high-order cross-modulation component will affect the minimum mean-square solution of the weight [16]. Thus the optimal solution cannot be achieved. With the acquisition error increasing, the effect of adaptive predistortion will be worse. It can be seen that reconstructing the missing fifth-order and higher-order intermodulation signals in the feedback loop has a great influence on the predistortion effect.

In addition, the requirement of the traditional digital predistortion method for the sampling rate of ADC and DAC is not only related to the bandwidth of the power amplifier output signal at the carrier frequency of two sub-bands, but also to the interval between two sub-bands. To capture the fifth-order in-band intermodulation and cross-modulation products, it is necessary to sample the signal whose output bandwidth is $(f_2 - f_1) + 5 \times 1.2\max(B_1, B_2)$. Therefore, in order to improve the predistortion effect and reduce the sampling rate, this paper proposes an undersampled digital predistortion system with high precision to reconstruct the missing fifth-order and the high-order signals, that is, using compressed sensing sampling in the predistortion feedback loop and (Adaptive Sparse) APSP algorithm to reconstruct the fifth-order intermodulation signal, which not only uses the compressed sensing characteristics to reduce sampling rate but also improves the precision of reconstructed signals to enhance the weight of coefficient estimation and improves the predistortion effect. In the Next section, this structure is introduced in detail.

2 ADAPTIVE FUSION OF DOUBLE FREQUENCY POWER AMPLIFIER UNDER SAMPLING PREDISTORTION

2.1 Adaptive New Undersampling Predistortion Model Structure

Fig. 2 is an overall undersampled dual-frequency predistortion structure, which consists of a dual-frequency piecewise functional memory effect compensator and a subsampled reconstructed feedback loop. The main conversion process of the dual-frequency piecewise function memory effect compensator is as follows: Its main components can be divided into a predistortion simplified model and a subsampled reconstructed feedback loop. The core idea of the predistortion simplification model is to combine a piecewise linear predistortion model with a lookup table [16].

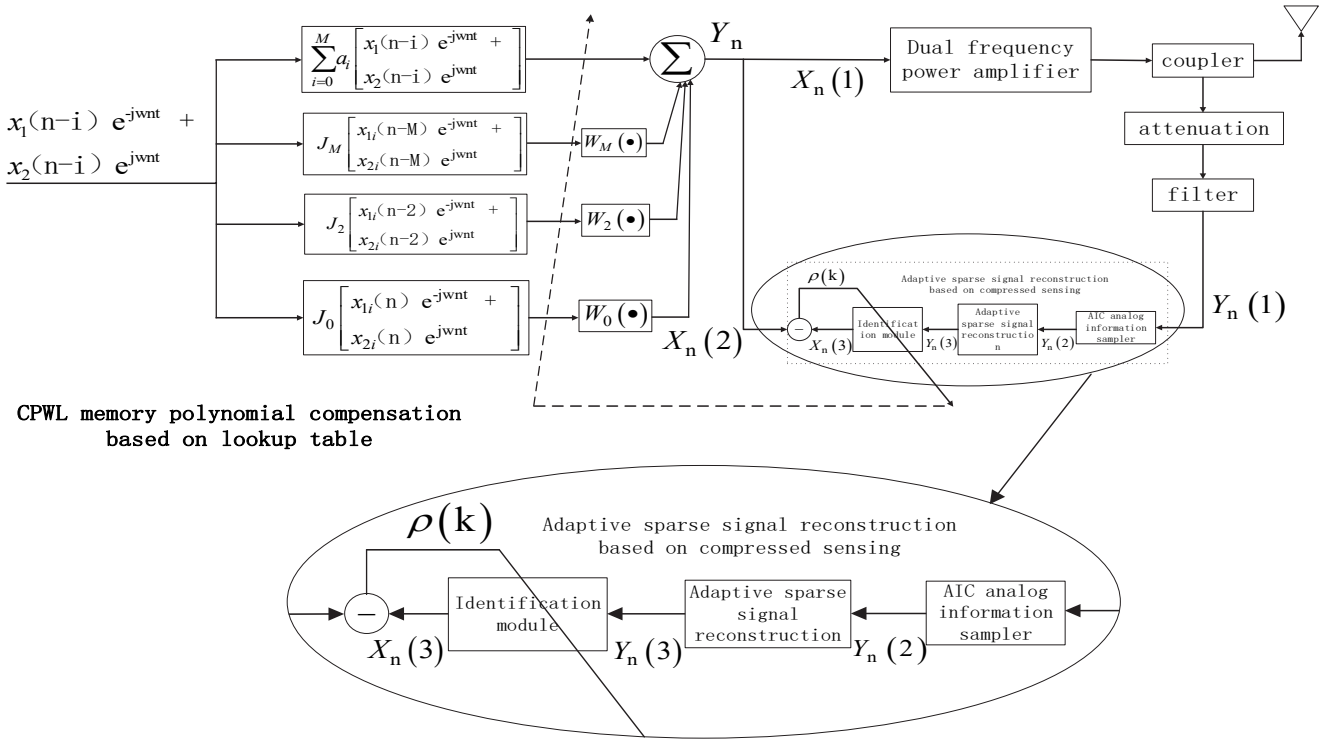

Figure 2 Undersampled dual-frequency predistortion structure

Because both CPWL function [17] and a polynomial function can be used to describe the non-linear characteristics of a power amplifier, it is assumed that polynomial function can approximate CPWL function by choosing the right of polynomial function, that is:

$$\sum_{r=1}^{R} b_{r,i} \left\| x_1(n-i)\mathrm{e}^{-j\omega nt} + x_2(n-i)\mathrm{e}^{j\omega nt} \right| - \beta_r \Big| \approx \approx \sum_{q=1}^{Q} \upsilon_{q,i} \left| x_1(n-i)\mathrm{e}^{-j\omega nt} + x_2(n-i)\mathrm{e}^{j\omega nt} \right|^q \tag{9}$$

The combination of the Eq. (9) and the lookup table is the Eq. (10), Fig. 2. In the solid box, the dual-frequency piecewise function power amplifier model is combined with the lookup table to simplify the coefficients. The CPLU memory polynomial compensation model based on the lookup table can be written as:

$$\sum_{q=1}^{Q} \upsilon_{q,i} \left| x_1(n-i)\mathrm{e}^{-j\omega nt} + x_2(n-i)\mathrm{e}^{j\omega nt} \right|^q \approx \approx LUT\left(\left| x_1(n-i)\mathrm{e}^{-j\omega nt} + x_2(n-i)\mathrm{e}^{j\omega nt} \right| \right) \tag{10}$$

$$y(n)=\sum_{i=0}^{M}a_i\left[x_1(n-i)\mathrm{e}^{-j\omega nt}+x_2(n-i)\mathrm{e}^{j\omega nt}\right]+$$
$$+b+\sum_{r=1}^{R}\sum_{i=0}^{M}b_{r,i}\left[x_1(n-i)e^{-j\omega nt}+x_2(n-i)\mathrm{e}^{j\omega nt}\right]\cdot \quad (11)$$
$$\cdot LUT\left(\left|x_1(n-i)\mathrm{e}^{-j\omega nt}+x_2(n-i)\mathrm{e}^{j\omega nt}\right|\right)$$

Among them, $x_1(n-i)\mathrm{e}^{-j\omega nt}+x_2(n-i)\mathrm{e}^{j\omega nt}$ and $y(n)$ are input signals and memory effect compensation signals, $J_i(\bullet)$ is a nonlinear function. $\upsilon_{q,i}$ is the coefficient of transmission function $W_i(\bullet)$. Q is the highest order of digital predistortion polynomial. M is the length of memory effect.

The final formula combined with the look-up table is:

$$y(n)=\sum_{i=0}^{M}a_i\left[x_1(n-i)\mathrm{e}^{-j\omega nt}+x_2(n-i)\mathrm{e}^{j\omega nt}\right]+$$
$$+\sum_{q=1}^{Q}\sum_{i=0}^{M}\upsilon_{q,i}\left[x_1(n-i)\mathrm{e}^{-j\omega nt}+x_2(n-i)\mathrm{e}^{j\omega nt}\right]\cdot$$
$$\cdot\left|x_1(n-i)\mathrm{e}^{-j\omega nt}+x_2(n-i)\mathrm{e}^{j\omega nt}\right|^q=$$
$$=\sum_{i=0}^{M}a_i\left[x_1(n-i)\mathrm{e}^{-j\omega nt}+x_2(n-i)\mathrm{e}^{j\omega nt}\right]+ \quad (12)$$
$$+\sum_{q=1}^{Q}\sum_{i=0}^{M}\upsilon_{q,i}J_i\left[x_1(n-i)\mathrm{e}^{-j\omega nt}+x_2(n-i)\mathrm{e}^{j\omega nt}\right]=$$
$$=\sum_{i=0}^{M}a_i\left[x_1(n-i)\mathrm{e}^{-j\omega nt}+x_2(n-i)\mathrm{e}^{j\omega nt}\right]+$$
$$+\sum_{i=0}^{M}W_i\left\{J_i\left[x_1(n-i)\mathrm{e}^{-j\omega nt}+x_2(n-i)\mathrm{e}^{j\omega nt}\right]\right\}$$

The other parts of the formula mainly apply the compressed sensing adaptive sparse reconstruction algorithm to the feedback loop of the predistortion system. In the predistortion feedback loop, compressed sensing sampling is used, and the (Adaptive Sparse) APSP algorithm is used to reconstruct the fifth order intermodulation signal. The input signal Q_n of the dual frequency power amplifier is divided by the coupler as shown in Fig. 2, passing through the main path and branch respectively. Input signal $X_n(1)$ on main path passes directly into dual frequency power amplifier. On the branch path, the signal reconstruction module based on compressed sensing obtains the output signal of the power amplifier in the under-sampling state, and reconstructs the original signal $X_n(3)$ before the under-sampling. That is to say, the filtered out-of-band fifth-order iso-high-order intermodulation distortion signal is reconstructed after passing through the signal reconstruction module. The compressed sensing algorithm in the reconstruction module adopts the (Adaptive Sparse) APSP algorithm. $\boldsymbol{P}$ is defined as a Gauss matrix, $Y_n(2)$ is an under-sampled output vector and $Y_n(3)$ is the fifth-order vector after reconstruction. The algorithm estimates the sparsity adaptively to achieve high-precision reconstruction when the sparsity is unknown. Aiming at the dual-frequency main signal, fifth-order and high-order out-of-band modulation signal, this paper considers signal fusion as a compression sensing problem, and reconstructs a complete signal by APSP algorithm. This method not only shows the undersampled predistortion structure, but also improves the reconstruction accuracy of the fifth-order signals outside the band. The effect of losing the fifth order equivalent signal on the minimum mean square solution of the weight in the identification algorithm is reduced, and the effect of the adaptive sparse predistortion structure is improved.

2.2 Signal Fusion and Adaptive Sparse Signal Reconstruction

2.2.1 Signal Fusion

In fact, multi-band signal fusion [18] is the fusion of continuous sampled signals of multi-frequency power amplifier in the working frequency band. This paper mainly focuses on the multi-frequency fusion of main signals output by predistortion structure and random sampling of all intermodulation signals in full band. It can be regarded as a single-frequency power amplifier is the fusion of sampled signals at a certain frequency point. If there is a g band power amplifier, its working frequency band sampling number is N_g (frequency band does not coincide), then for full-band random sampling, it is equivalent to having N_g single-band power amplifiers, and each single-band power amplifier randomly picks a frequency point in the full-band (sampling does not repeat), so the two are essentially equivalent. The output signal with the fifth-order intermodulation satisfies K-sparsity and compressibility, and the full-band random sampling number is less than the full-band sampling number, under the circumstances that the sample matrix is random. Moreover, the purpose of signal fusion is to recover the full-band signal from fewer observations. Therefore, the full band random sampling multi- frequency signal fusion problem is equivalent to the compressed sensing [19] problem. The missing out-of-band fifth-order and high-order intermodulation signals are obtained by adaptive sparsity reconstruction of the fused signals. The sampling and reconstruction processes of compressed sensing are as follows.

2.2.2 Adaptive Sparse Signal Reconstruction

In [20], the starting value of sparsity is set to (0 - 0.1) M according to the reconstruction condition M >KlogN (where M and N are rows and columns of measurement matrix $\boldsymbol{P}$ and K is sparsity). The proposition is verified in [21]: Let measurement matrix $\boldsymbol{P}$ satisfy RIP (Restricted Isometry Property) finite isometric property with parameter (K,δ_K), that is, if $\boldsymbol{P}$ satisfies:

$$(1-\delta_{\mathrm{k}})\left\|Y_n(2)\right\|_2^2<\left\|\boldsymbol{P}Y_n(2)\right\|_2^2\le(1+\delta_{\mathrm{k}})\left\|Y_n(2)\right\|_2^2 \quad (13)$$

where $Y_n(2)$ is K sparse signal, if $\delta_{\mathrm{k}}<1$, then the measurement matrix $\boldsymbol{P}$ satisfies K order RIP. If $K_0\ge K$,

that is, the estimate of sparsity is greater than the true value, the condition $\left\|\boldsymbol{P}_{I^0}^{T} Y_n(3)\right\|_2 \geq \frac{1-\delta_K}{\sqrt{1+\delta_K}}\left\|Y_n(3)\right\|_2$ is established. Thresholds T_1 and T_2 are set in [23] to reduce the energy difference to a faster and slower stage: greater than T_1 is the region with larger energy difference, that is, when the energy difference between reconstructed signals in two adjacent stages is $\left\|\hat{Y_n}(2)-\hat{Y_{n-1}}(2)\right\|_2 > T_1$. Increasing step size reduces the reconstructed time. If the energy difference is greater than T_2 and less than T_1, that is to say, when the energy difference of the reconstructed signal is $T_2 < \left\|\hat{Y_n}(2)-\hat{Y_{n-1}}(2)\right\|_2 \leq T_1$ in two adjacent stages, the step size is reduced and the reconstruction accuracy is improved. According to a large number of experimental results. T_1 is:

$$\lg(s)(N/M)^4 \mathrm{e}^{-5}\left\|\hat{Y_{n-1}}(2)\right\|_2 \tag{14}$$

T_2 is:

$$0.2\lg(s)(N/M)^4 \mathrm{e}^{-5}\left\|\hat{Y_{n-1}}(2)\right\|_2 \tag{15}$$

To reduce the possibility of over estimation, we choose step size S initial value as $S_0 = M/\left[2\log_2(N)\right]$, the size of the measurement matrix $\boldsymbol{P}$ is 2048 × 1024 Gaussian matrix. According to the above conditions, this paper proposes an adaptive sparsity estimation algorithm for feedback loop signals in the indirect learning predistortion structure. The sparse estimation value of sparse representation can be obtained by LS algorithm, and its energy is arranged from large to small. The first L components with large energy are selected, and their corresponding index values are stored in set J.

Algorithmic flow: Firstly, according to the condition of compressed sensing reconstruction, setting the appropriate sparsity starting value K_0 can reduce the number of iterations. Secondly, the relationship between the starting value K_0 and the true value K is judged. When $\left\|\boldsymbol{P}_{I^0}^{T} Y_n(3)\right\|_2 \geq \frac{1-\delta_K}{\sqrt{1+\delta_K}}\left\|Y_n(3)\right\|_2$, $K_0 \geq K$, the adaptive sparsity algorithm to prevent over-estimation or under-estimation. Finally, when the initial value is smaller than the real value, a step S is added to the initial value. Otherwise, reduce the step size S. When the step S is selected, the reconstruction time can be dynamically adjusted according to the energy difference between the reconstructed signals in the two adjacent stages. Firstly, an initial value of S is given. If the energy of adjacent signal satisfies $\left\|\hat{Y_n}(2)-\hat{Y_{n-1}}(2)\right\|_2 > T_1$, the step size needs to be increased by half. If the energy of adjacent signal satisfies $T_2 < \left\|\hat{Y_n}(2)-\hat{Y_{n-1}}(2)\right\|_2 \leq T_1$, it means that the difference energy between the adjacent two stages is small, and it need to have the step size. Adaptive sparse signal reconstruction by Adaptive Sparse algorithm. The flow chart is as follows:

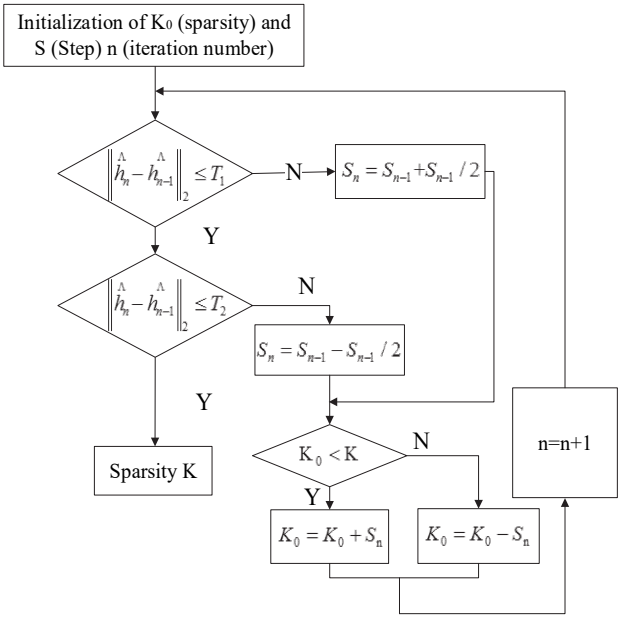

Figure 3 Flow chart of adaptive sparsity algorithm

3 HARDWARE PLATFORM EXPERIMENTAL RESULTS AND ANALYSIS

In order to verify the effectiveness of the proposed method, the test power amplifier is class F power amplifier $\left(V_{\mathrm{ds}} = 28v,\ V_{\mathrm{gs}} = -5v\right)$ of 30W. The dual-frequency input signal is a WCDMA signal with a center frequency of 2.61 GHz and an LTE signal with a center frequency of 2.69 GHz. The signal bandwidth is 20 MHz. The average output power is about 32 dBm and the efficiency is 44.2%. The sampling rate in the sampling structure $f_s = 50$ MHz. The test platform is built as shown in Fig. 3. The digital baseband I and Q orthogonal components generated by ADS (Advanced Design System) are processed by the dual-frequency piecewise function model memory effect compensator, and then the input excitation signals of concurrent dual-frequency power amplifiers are generated by the modulation and up-conversion functions of AgilentMAX N5182A. Then the power amplifier is stimulated by the radio frequency signal obtained through modulation and up-conversion in the signal generator. After coupling, 40 dB attenuation, filtering and compression sensing sampling reconstruction, the output signal of power amplifier is sent to the spectrum analyzer for down conversion and demodulation. The output signal of the spectrum analyzer is captured by the MATLAB. The output of the power amplifier is synchronized with the corresponding original input signal for updating the coefficient of the behavioral model.

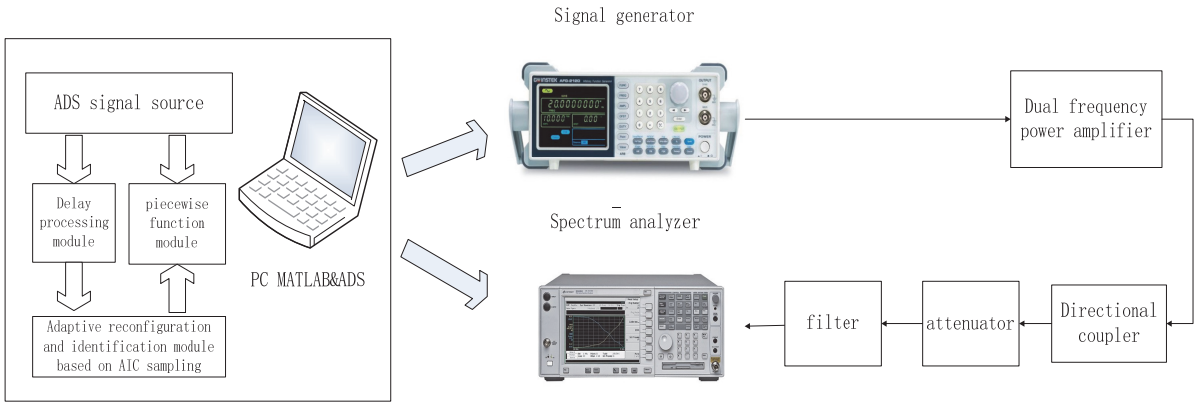

Figure 4 Compressed sensing under-sampling digital predistortion verification platform

3.1 Reconstruction Performance of Adaptive Sparse Algorithm

3.1.1 Five and Higher Order Signal Reconstruction Accuracy

Around the reconstruction of signal distortion SNR (Signal-to-noise ratio) is compared as follows. x_{true} and x_{rec} are the pre-reconstruction signal and the post-reconstruction signal respectively.

$$SNR\left(x_{true}, x_{rec}\right) = 20\lg \frac{\left\|x_{true}\right\|_2}{\left\|x_{true} - x_{rec}\right\|_2} \tag{16}$$

The SNR curves before and after reconstruction are shown in Fig. 5. The SNR before iteration is about 50 dB, and after about 12 iterations, the SNR reaches about 250 dB. The SNR results show that this method can be applied to all-digital predistortion and to linearize the power amplifier in under-sampling.

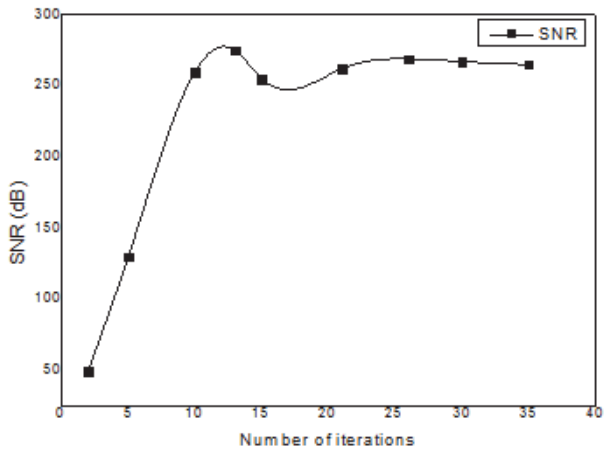

Figure 5 SNR iteration curve (before and after reconstruction)

3.1.2 Complexity of Refactoring Algorithm

For a Gauss matrix whose size is 2048 × 1024, the computational complexity is $O(12 \times 2048 \times 1024)$. Because sparse random matrix contains a large number of zero elements. When the number of measurements required for accurate reconstruction increases slightly, the measurement and reconstruction time can be greatly shortened. After removing zero elements, the complexity of the simulation is reduced to $O(12 \times 512 \times 256)$, which is of practical significance for the large amount of Data operation. The reduction is $O(12 \times 512 \times 256)$, and has practical significance for large data computation.

3.2 Adaptive Reconstruction of Dual Frequency Predistortion Based On Compressed Sensing

The performance of the general evaluation digital predistortion is the (Adjacent Channel Power Radio) *ACPR* and the normalized mean square error *NMSE*. *ACPR* is defined as the power ratio of adjacent channel output and in band carrier:

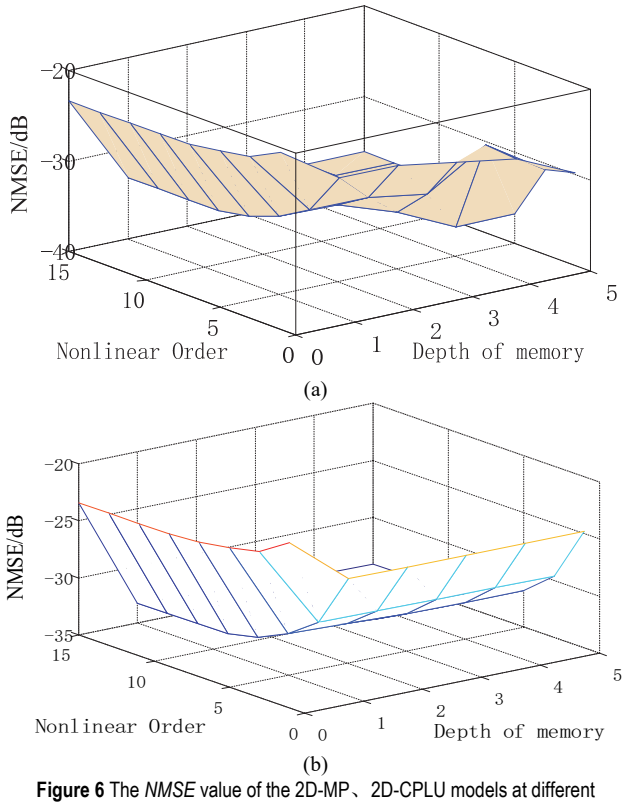

Figure 6 The *NMSE* value of the 2D-MP、2D-CPLU models at different parameters: **(a)** The *NMSE* value of the 2D-MP model at different parameters, **(b)** The *NMSE* value of the 2D-CPLU model at different parameters

$$ACPR_{dBc} = 10\lg\left(\frac{\int_{f_{neighbor}} Y(f)\mathrm{d}f}{\int_{f_{main}} Y(f)\mathrm{d}f}\right) \tag{17}$$

Among them, $Y(f)$ is the power spectrum density, $f_{neighbor}$ is the adjacent channel signal frequency, and f_{main} is the main frequency channel.

The normalized mean square error *NMSE* is:

$$NMSE_{dB} = 10\lg\left[\frac{\sum_{\alpha=1}^{\beta}\left|y_{measure}(\alpha)-y_{mod\,el}(\alpha)\right|^2}{\sum_{\alpha=1}^{\beta}\left|y_{measure}(\alpha)\right|^2}\right] \quad (18)$$

Among them, $y_{measure}(\alpha)$ is the input measurement signal, $y_{model}(\alpha)$ is the dual frequency power amplifier output signal, and β is the sampling point.

In order to obtain the appropriate memory depth to verify the performance of the model *M* and the nonlinear order *Q*, using Matlab software to calculate the 2D-CPLU model scanning *Q* from 0 to 15 and scanning *M* from 0 to 5 to get the NMS E value shown in Fig. 7.

The *NMSE* indexes of the 2D-MP model and the 2D-CPLU model increase with the increasing of non-linear order and memory depth, but at the same time, the coefficients of the model increase significantly. When the non-linear order and memory depth are both maximized, the corresponding index values of the model are the lowest, but the model coefficients introduced at this time are also large. When the memory depth and linear order increase to a certain value, the improvement of *NMSE* index caused by the continuous improvement of memory depth or non-linear order is not obvious, but leads to the number of coefficient with a sharp increasing. Considering the accuracy of the model and the coefficients of the model, the best memory depth to use is 2 and the best non-linear order is 5.

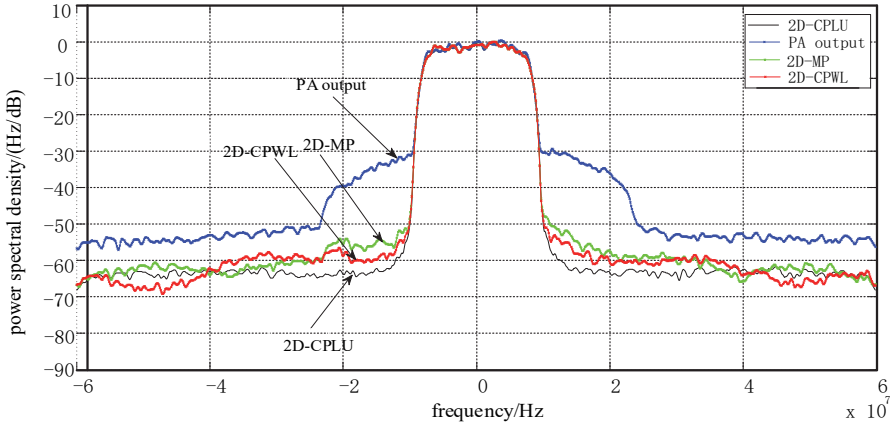

Figure 7 Comparison of the pre-distortion spectrum of each model at *f*1 frequency

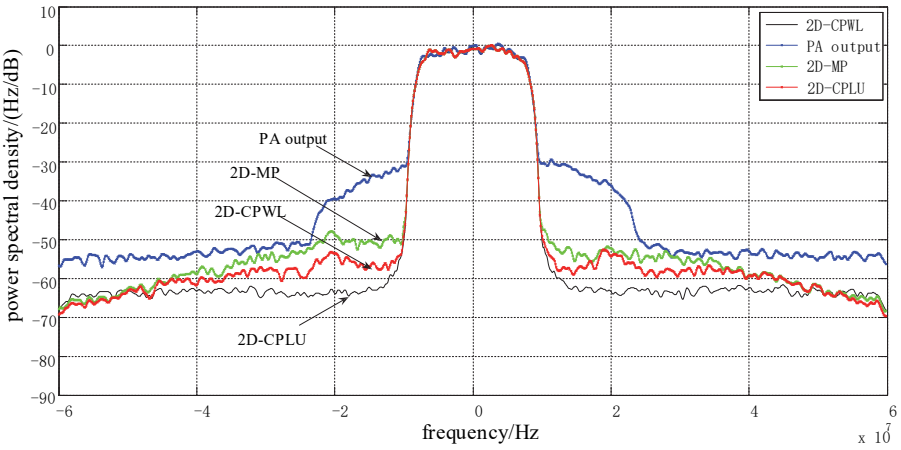

Figure 8 Comparison of the pre-distortion spectrum of each model at *f*2 frequency

In order to facilitate the comparison of model performance, the 2D-MP model [19] the 2D-CPWL, and 2D-CPLU models were also tested. The test results are shown in Fig. 7 (Frequency 1) and Fig. 8 (Frequency 2). According to the graph, the dual-frequency digital predistortion model based on CPWL function is superior to the polynomial-based 2D-MP, 2D-CPWL and 2D-CPLU models to achieve considerable linearization performance. When the average output power of dual-frequency power amplifier falls back about 1 dB, the normalized test results of the power spectrum are shown in Fig. 7 and Fig. 8. The adjacent channel leakage power ratio (ACLR) of a power amplifier processed by traditional digital predistortion technology is about 25 dBc. After using the under-sampling predistortion technology in this paper, the ACLR index can be improved to 45 dBc, which is close to the ideal linear power amplifier index. It is shown from the graph that the 2D-CPLU model proposed which is based on achieves a good predistortion effect.

To verify the model performance, Tab. 1 shows the performance of output power, *ACPR*, *NMSE* between the predistortion models of 2D-MP, 2D-CPWL and 2D-CPLU.

Table 1 Performance and number comparison of *ACPR* and *NMSE* in different predistortion models

Model	*f*1				*f*2			
	Power / dBm	*ACPR* / dBc	*NMSE* / dB	Sum of parameters	Power / dBm	*ACPR* / dBc	*NMSE* / dB	Sum of parameters
initial	32.8	−34.02/−33.8	−26.2		32.8	−33.90/−34.7	−26.49	
2D-MP	32.5	−40.8/−40.5	−37.49	90	32.6	−40.40/−41.9	−37.91	90
2D-DDR	32.5	−43.67/−44.5	−38.36	79	32.6	−43.65/−44.29	−38.87	79
2D-CPWL	32.5	−45.89/−45.9	−38.47	66	32.6	−45.83/−46.79	−39.2	66
2D-CPLU	32.5	−49.92/−49.8	−40.02	42	32.6	−49.86/−50.6	−40.12	42

The *ACPR* (Adjacent Channel Power Radio) of the concurrent dual-frequency power amplifier is about −34.02 dBc before the linearization, but after the self-adaptive sparse reconstruction pre-distortion structure proposed in this paper, the output power of the power amplifier only needs to be rolled back by 1 dB. The *ACPR* can be improved to −49.92 dBc. The *ACPR* parameter rise to 91 dB.

By comparing the output power of power amplifier and *ACPR*, *NMSE*, it can be seen that the linearization performance of 2D-CPWL is better than 2D-MP and 2D-DDR. In different pre-distortion models, the *NMSE* performance of the 2D-CPLU model is improved by about 2 - 3 dB compared with the other three models. Moreover, there is no need to extract phase like 2D-DDR, so the 2D-CPLU model is more stable.

This paper proposed a predistortion structure of adaptive reconstruction based on compression sensing, with the frequency of power amplifier at f_1, and the input and output signal constellations of nonlinear odd order were shown in Fig. 9. In Fig. 9b where pre-distortion has not been introduced, the output signal constellation has severe distortion. Comparing the under-sampling predistortion method presented in this paper is in Fig. 9d with the traditional predistortion in Fig. 9c. Even though Fig. 9c has obvious compensation for distortion, Fig. 9d is more accurate to reconstruct the fifth-order signal and more accurate to describe the characteristics of power amplifier. The input and output signal constellation of the method proposed achieves good consistency.

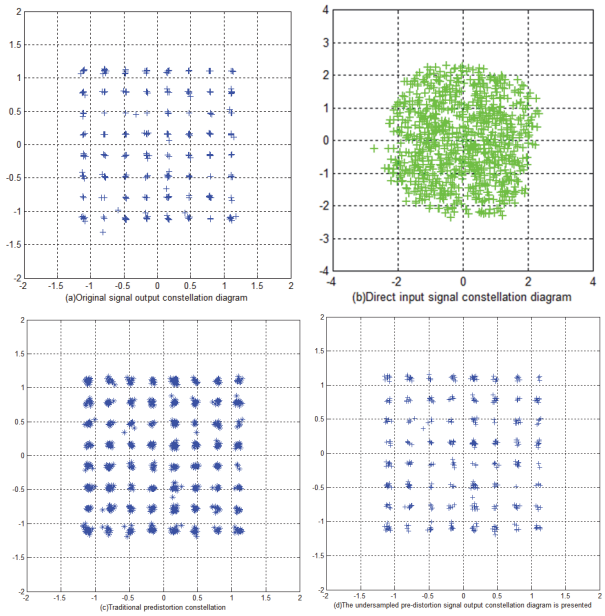

Figure 9 Power spectral density under different predistortion (a) Constellation diagram of original signal output (b) Signal Constellation of Direct Power Amplifier (c) Traditional predistortion signal constellation (d) The output constellation of under-sampled predistortion signal

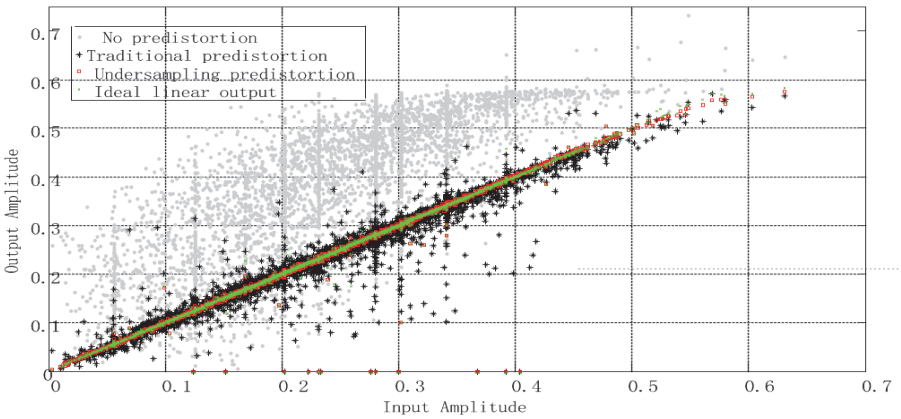

Figure 10 AM/AM characteristics of dual-frequency amplifier

To verify the effectiveness of the proposed method of power amplifier linearization system, the AM/AM characteristics and AM/PM characteristics of the output signal are simulated under the same signal feedback sampling rate. The results are shown in Fig. 10. In this paper, a random demodulation method is introduced for comparative analysing. It can be seen that the traditional predistortion method has obvious distortion when the sampling bandwidth is less than the signal bandwidth. The adaptive reconstructed predistortion method based on compressed sensing achieves better linearization performance. Using compressed sensing sampling in the predistortion feedback loop and using an (Adaptive Sparse) APSP algorithm reconstructs the fifth order intermodulation signal. This method improves the precision of reconstructed signal, the weight of coefficient estimation and the predistortion effect. Moreover, it is more flexible and accurate than the traditional predistortion method.

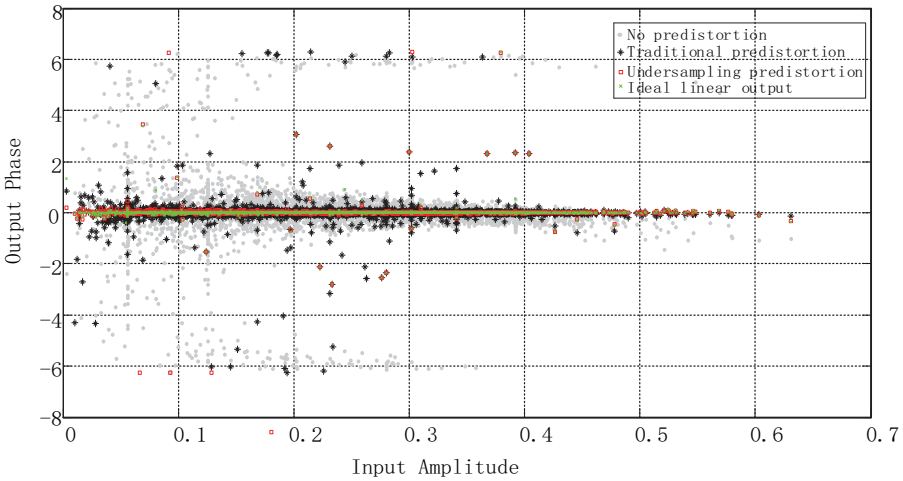

Figure 11 AM/PM characteristics of dual-frequency amplifier

4 CONCLUSION

In this paper, a dual frequency predistortion adaptive sparse signal reconstruction algorithm is proposed. In the pre-distortion feedback loop, compressed sensing sampling and the (Adaptive Sparse) APSP algorithm are used to reconstruct the fifth-order intermodulation signal. The simulation results show that *NMSE* improves about 2-3 dB compared with 2D-MP, 2D-CPWL and 2D-CPLU models. The output power of dual-frequency power amplifier can be improved to 49 dBc by only 1 dB back, and good predistortion effect can be obtained. This structure not only improves the reconstructed signal accuracy, enhancing the coefficient estimation weight, and improving the pre-distortion effect, but also reduces the sampling bandwidth. It is of great significance to reduce the predistortion sampling rate and improve the linearity of power amplifier.

Acknowledgements

We thank the anonymous reviewers for their feedback and comments. This study was supported by the National Fund: Cognitive Radio System Power Amplifier Design Modeling and Predistortion Research under the Compressed Sensing Framework (61701211), Beijing Science and Technology Project: Hardware-accelerated 3D reconstruction sports display platform (Z201100005820010), Horizontal subject of Liaoning Technical University: Research on Image Transmission and Reconstruction Technology Based on Compressed Sensing (21-2067) and Liaoning province Department of Education fund (No. LJ2019QL011).

5 REFERENCES

[1] Hui, M. (2013). *Research on digital predistortion linearization technology of concurrent multiband multimode RF power amplifier.* Doctoral dissertation, Ningbo University. https://kns.cnki.net/KCMS/detail/detail.aspx?dbname =CDFD1214&filename=1014030345.nh

[2] Wolff, N., Heinrich, W., & Bengtsson, O. (2017). Highly Efficient 1.8-GHz Amplifier With 120-MHz Class-G Supply Modulation. *IEEE Transactions on Microwave Theory and Techniques*, *65*(12), 5223-5230. https://doi.org/10.1109/tmtt.2017.2769089

[3] Zhao, J. M. (2017). *Research on Digital Predistortion Technology of RF Power Amplifier in Wireless Communication*. Doctoral dissertation, Beijing University of Posts and Telecommunications. https://kns.cnki.net/KCMS/detail/detail.aspx?dbname=CDFDLAST2018&filename=1017289455.nh

[4] Xiang, H. X., Yu, C. P., Gao, J. C., Li, S. L., Wu, Y. L., Su, M., & Liu, Y. A. (2013). Dynamic deviation reduction-based concurrent dual-band digital predistortion. *International Journal of RF and Microwave Computer-Aided Engineering*, *24*(3), 401-411. https://doi.org/10.1002/mmce.20773

[5] Roblin, P., Myoung, S. K., Chaillot, D., Kim, Y. G., Fathimulla, A., Strahler, J., & Bibyk, S. (2008). Frequency-Selective Predistortion Linearization of RF Power Amplifiers. *IEEE Transactions on Microwave Theory and Techniques*, *56*(1), 65-76. https://doi.org/10.1109/tmtt.2007.912241

[6] Kim, J., Roblin, P., Yang, X., & Chaillot, D. (2012). A new architecture for frequency-selective digital predistortion linearization for RF power amplifiers. *2012 IEEE/MTT-S International Microwave Symposium Digest. Montreal, QC, Canada.* https://doi.org/10.1109/mwsym.2012.6259731

[7] Cidronali, A., Magrini, I., Fagotti, R., & Manes, G. (2008). A new approach for concurrent Dual-Band IF Digital PreDistortion: System design and analysis. *2008 Workshop on Integrated Nonlinear Microwave and Millimetre-Wave Circuits.Malaga, Spain.* https://doi.org/10.1109/inmmic.2008.4745733

[8] Bassam, S. A., Helaoui, M., & Ghannouchi, F. M. (2011). 2-D Digital Predistortion (2-D-DPD) Architecture for Concurrent Dual-Band Transmitters. *IEEE Transactions on Microwave Theory and Techniques*, *59*(10), 2547-2553. https://doi.org/10.1109/tmtt.2011.2163802

[9] Ma, Y. Q. (2017). *Research on Wideband Digital Receiver Based on Compressed Sensing*. Master's thesis, University of Electronic Science and Technology. https://kns.cnki.net/KCMS/detail/detail.aspx?dbname=CMFD201801&filename=1017078371.nh

[10] Sharma, S. K., Lagunas, E., Chatzinotas, S., & Ottersten, B. (2016). Application of Compressive Sensing in Cognitive Radio Communications: A Survey. *IEEE Communications Surveys & Tutorials*, *18*(3), 1838-1860. https://doi.org/10.1109/comst.2016.2524443

[11] Zhang, Y. K., Wang, H. Y., Li, G., & Liu, F.L. (2017). A concurrent dual-frequency digital predistortion model based on piecewise linear function.*2017 National Microwave and Millimeter Wave Conference Proceedings*, *2*. https://kns.cnki.net/kcms/detail/detail.aspx?FileName=ZDWB201705003081&DbName=CPFD2017

[12] Chua, L. & Deng, A. (1988). Canonical piecewise-linear

representation. *IEEE Transactions on Circuits and Systems*, *35*(1), 101-111. https://doi.org/10.1109/31.1705

[13] Zhu, A. (2015). Decomposed Vector Rotation-Based Behavioral Modeling for Digital Predistortion of RF Power Amplifiers. *IEEE Transactions on Microwave Theory and Techniques*, *63*(2), 737-744. https://doi.org/10.1109/tmtt.2014.2387853

[14] Zhang, L. & Feng, Y. (2015). Dual-band digital predistortion method for combined structure design. *Computer Applied Research*, *32*(07), 2133-2135. Retrieved from https://kns.cnki.net/kcms/detail/detail.aspx?FileName=JSYJ201507052&DbName=CJFQ2015

[15] Hu, X., Wang, J. K., Liu, F., Ou, L.J., Liang, J., Wang, G., & Luo, J. R. (2016). Research on undersampling predistortion based on compressed sensing. *Journal of Communications*, *37*(11), 74-79. https://kns.cnki.net/kcms/detail/detail.aspx?FileName=TXXB201611009&DbName=CJFQ2016

[16] Cuprak, T. D. & Wage, K. E. (2017). Efficient Doppler-Compensated Reiterative Minimum Mean-Squared-Error Processing. *IEEE Transactions on Aerospace and Electronic Systems*, *53*(2), 562-574. https://doi.org/10.1109/taes.2017.2651480

[17] Jia, B., Zhao, Y., Liu, K. H., Ma, Y. T., & Liu, Y. B. (2017). Power amplifier model based on piecewise linear function and digital predistortion application. *Computer Engineering and Science*, *39*(11), 2043-2048. Retrieved from https://kns.cnki.net/kcms/detail/detail.aspx?FileName=JSJK201711012&DbName=CJFQ2017

[18] Ye, F., He, F., Liang, D. N., & Zhu, J. B. (2010). Multi-frequency signal fusion based on compressed sensing. *Journal of National Defense University of Science and Technology*, *32*(04), 84-87.Retrieved from https://kns.cnki.net/kcms/detail/detail.aspx?FileName=GFKJ201004017&DbName=CJFQ2010

[19] Yu, X., Zheng, H. B., & Zeng, Y. Q. (2016). Adaptive weighted matching tracking algorithm based on compressed sensing. *Journal of Chongqing University of Posts and Telecommunications (Natural Science Edition)*, *28*(05), 707-712. https://kns.cnki.net/kcms/detail/detail.aspx?FileName=CASH201605015&DbName=CJFQ2016

[20] Zhou, C. M. (2010). *Research on signal reconstruction algorithm based on compressive sensing*. Master's thesis, Beijing Jiaotong University. https://kns.cnki.net/KCMS/detail/detail.aspx?dbname=CMFD2010&filename=2010119669.nh

[21] Yang, C., Feng, W., Feng, H., Yang, T., & Hu, B. (2010). A sparse adaptive subspace tracking algorithm in compressed sampling. *Acta Electronica Sinica*, *38*(08), 1914-1917. https://kns.cnki.net/kcms/detail/detail.aspx?FileName=DZXU201008031&DbName=CJFQ2010

[22] Gao, R., Zhao, Z. R., & Hu, S. H. (2010). Variable Step Size Adaptive Matching Pursuit Algorithm for Image Reconstruction Based on Compressive Sensing. *Acta Optica Sinica*, *30*(6), 1639-1644. https://doi.org/10.3788/aos20103006.1639

[23] Zhang, Q., Liu, S., Gong, D., & Tu, Q. (2019). A Latent-Dirichlet-Allocation Based Extension for Domain Ontology of Enterprise's Technological Innovation. *International Journal of Computers Communications & Control*, *14*(1), 107-123. https://doi.org/10.15837/ijccc.2019.1.3366

[24] Ma, Y., Zhang, Z., Ihler, A., & Pan, B. (2018). Estimating Warehouse Rental Price using Machine Learning Techniques. *International Journal of Computers Communications & Control*, *13*(2), 235-250. https://doi.org/10.15837/ijccc.2018.2.3034

[25] Ma, Y., Zhang, Z., & Ihler, A. (2020). A Deep Choice Model for Hiring Outcome Prediction in Online Labor Markets. *International Journal Of Computers Communications & Control*, *15*(2). https://doi.org/10.15837/ijccc.2020.2.3760

[26] Yu, W., Hou, G., Xia, P. & Li, J. (2019). Supply Chain Joint Inventory Management and Cost Optimization Based on Ant Colony Algorithm and Fuzzy Model. *Technical Gazette*, *26*(6), 1729-1737. https://doi.org/10.17559/TV-20190805123158

[27] Qian, Y., Zeng, J., Zhang, S., Xu, D. & Wei, X. (2020). Short-Term Traffic Prediction Based on Genetic Algorithm Improved Neural Network. *Technical Gazette, 27*(4), 1270-1276. https://doi.org/10.17559/TV-20180402112949

[28] Saric, T., Vukelic, D., Simunovic, K., Svalina, I., Tadic, B., Prica, M. & Simunovic, G. (2020). Modelling and Prediction of Surface Roughness in CNC Turning Process using Neural Networks. *Technical Gazette, 27*(6), 1923-1930. https://doi.org/10.17559/TV-20200818114207

[29] Bilhan, A. K & Sunter, S. (2020). Simulation and Design of Three-Level Cascaded Inverter Based on Soft Computing Method. *Technical Gazette*, *27*(2), 489-496. https://doi.org/10.17559/TV-20180503115747

Contact information:

Mingming GAO, PhD, Associate Professor
1) School of Information Science and Technology, Dalian Maritime University, No. 1 Linghai Road, Ganjingzi District, Dalian, Liaoning Province, China,
2) School of Electronics and Information Engineering, Liaoning Technical University, No.188 Longwan South Street, Xingcheng, Huludao, Liaoning Province, China
E-mail: gaomingming2080@163.com

Shaojun FANG, PhD, Full Professor
(Corresponding Author)
School of Information Science and Technology,Dalian Maritime University, No. 1 Linghai Road, Ganjingzi District, Dalian,Liaoning Province, China
E-mail: fangshj@dlmu.edu.cn

Jinling WANG, M.S.
School of Electronics and Information Engineering, Liaoning Technical University, No.188 Longwan South Street, Xingcheng, Huludao, Liaoning Province, China
E-mail: 3083884946@qq.com

Xueman ZHANG, M.S.
School of Electronics and Information Engineering, Liaoning Technical University, No.188 Longwan South Street, Xingcheng, Huludao, Liaoning Province, China
E-mail: 910389432@qq.com

Yuan CAO, PhD, Lecturer
School of Electrical and Control Engineering, Liaoning Technical University, No.188 Longwan South Street, Xingcheng, Huludao, Liaoning Province, China
E-mail: caoyuan0915@126.com